

## Optical and Structure Properties of $Mg_xZn_{1-x}O$ Thin Films by Pulsed Laser Deposition

Dr. Adawiya J. Haidar \* & Gehan E. Simon \*

Received on: 23/11/2008

Accepted on: 4/6/2009

### Abstract

In this study, the optical and structure properties of  $Mg_xZn_{1-x}O$  thin films is reported. The  $Mg_xZn_{1-x}O$  thin films were prepared on Glass substrates by Q-switch second harmonic Nd:YAG laser deposition technique with wavelength of 532nm from a ZnO target mixed with Mg of (0-0.3) wt% , and the films deposited at temperature (250°C).

The optical properties were characterized by transmittance and absorption spectroscopy measurements. For all the films the average transmission in the U.V (200-900) nm wavelength region was over 85% and the absorption edge shifted to a shorter wavelength as the magnesium concentration increased. The optical energy gap of  $Mg_xZn_{1-x}O$  thin films, measured from transmittance spectra could be controlled between (3.3eV and 4.2eV) by adjusting magnesium concentration. X-ray diffraction was used to investigate the structure of the film. The refractive index of hexagonal  $Mg_xZn_{1-x}O$  thin films decreases with the Mg concentration increase, such as at the wavelength of (500nm) the refractive index decreases from 1.93 to 1.85 as x increase from 0.15 to 0.3. The extinction coefficient and the complex dielectric constant were also investigated.

**Keywords:** Zinc oxides; Pulsed laser deposition; optical properties; MgZnO

### دراسة الخصائص البصرية و التركيبية لاغشية $Mg_xZn_{1-x}O$ بالترسيب بالليزر

#### الخلاصة

تم في هذا البحث دراسة الخصائص البصرية و التركيبية لاغشية  $Mg_xZn_{1-x}O$ . وتم تحضير الاغشية على قواعد زجاجية من خلال خلط اوكسيد الخارصين و المغنيسيوم بنسب وزنية مختلفة تتراوح بين (0-0.3)wt% باستخدام الترسيب بالليزر النديميوم اليك النبضي العامل بتقنية مفتاح عامل النوعية لتوليد التوافق الثاني ذو الطول الموجي (532)nm, رسبت الاغشية عند درجة حرارة (250°C). تم دراسة الخصائص البصرية بقياس طيفي النفاذية و الامتصاص . ان معدل النفاذية لكل الاغشية بالمنطقة فوق البنفسجية للاطوال الموجية بين (200-900) nm فوق 85% و تزداد حافة الامتصاص باتجاه الاطوال الموجية الاقصر بزيادة تركيز المغنيسيوم. وكانت فجوة الطاقة البصرية لاغشية  $Mg_xZn_{1-x}O$  المقاسة من طيف النفاذية بين (3.3-4.2) eV والتي يمكن السيطرة عليها بتغيير تركيز المغنيسيوم. تم دراسة التركيب البلوري للفيلم المرسب باستخدام اشعة X-ray. يقل معامل الانكسار لاغشية  $Mg_xZn_{1-x}O$  بزيادة تركيز المغنيسيوم, مثلا يقل معامل الانكسار من 1.93 الى 1.85 عند الطول الموجي 500nm بزيادة x من 0.15 الى 0.3, كذلك تم دراسة معامل الخمود و ثابت العزل.

## Introduction

ZnO, a II-VI oxide semiconductor with a direct wide band-gap of ~ 3.3 eV at room temperature is of immense interest now days for optoelectronic applications in UV-Blue spectral range [1,2]. The high cohesive energy of ZnO which is ~ 1.89 eV makes it a highly stable and perhaps the most radiation hard material amongst the direct band gap semiconductor family, which ensure a long life and a high degradation threshold of ZnO based optoelectronic devices. The high melting and boiling points of ZnO allow one to explore variety of heat treatments required for alloying purposes and device formation.

One of the most exciting features of ZnO is the stability of its excitons, which have a binding energy of ~ 60 meV [3]. Such a high binding energy of excitons allows one to realize excitonic absorption and recombination even at room temperature. Recently stimulated emission and lasing action due to excitonic recombination at a very low threshold has been reported by optically pumping the highly c-axis oriented thin ZnO film grown on (0001) Sapphire substrate using Pulsed Laser Deposition technique [4].

A crucial step in designing modern optoelectronic devices is the realization of band-gap engineering to create barrier layers and quantum wells in device heterostructures. In order to realize such optoelectronic devices, two important requirements should be satisfied, one is *p*-type doping of ZnO, and the other is modulation of the band gap. While *p*-type doping of ZnO is under intensive study, the latter has been

demonstrated by the development of Mg<sub>x</sub>Zn<sub>1-x</sub>O and Cd<sub>y</sub>Zn<sub>1-y</sub>O alloys, allowing modulation of band gap in a wide range [5-7]. In CdZnO the band gap is shifted to lower energies and in MgZnO to higher energies compared to ZnO [8-10]. CdO and MgO have the rocksalt crystal structure, while ZnO crystallizes in wurtzite structure. Mg<sub>x</sub>Zn<sub>1-x</sub>O crystallizes in wurtzite structure for  $x < 0.5$  and in rocksalt structure for  $x > 0.5$ . The ionicity of the Zn-O bonds compared with the Mg-O bonds are lower. Therefore, for Mg<sub>x</sub>Zn<sub>1-x</sub>O with high Mg content one expects high exciton binding energies, which should increase by increasing the Mg content in the crystal [11].

The variable bandgap energy provides the ability to adjust the operating wavelength of the devices. The alloying of Mg-ZnO to make Mg<sub>x</sub>Zn<sub>1-x</sub>O can increase the bandgap energy from 3.3 eV for ZnO to 7.8 eV for MgO (at high concentration of Mg) with relatively small mismatching (0.1%) in bond lengths of ZnO and MgO [12,13].

## 2. Experimental procedure

Mg<sub>x</sub>Zn<sub>1-x</sub>O thin films were synthesized by pulsed laser deposition system using a second harmonic Nd:YAG laser. Thin films were grown in a vacuum chamber with background pressure of  $\sim 1 \times 10^{-3}$  mbar. The Nd:YAG laser was operated at the wavelength of ( $\lambda = 533$  nm) with the repetition rate of (10Hz) and pulse duration of (7ns). The target to substrate distance was (3cm). Mg-ZnO composite targets with (Mg)<sub>x</sub>(Zn)<sub>1-x</sub> (for  $x = 0.15, 0.2$  and  $0.3$ ) were used during the deposition. The composite targets were obtained by the standard pressing and sintering method. Mg

and ZnO powders were first weighted and mixed with corresponding concentrations in methanol by magnetic blender for 1 hour. After the liquid was dry out, the mixed powder was blended mechanically again so that the mixture is uniformly distributed. The mixture was then calcined at 100 °C in flowing oxygen for 6 hours. The resultant powder was ground again and was pressed into round pellets with two-inch diameter. The targets were finally obtained after the pellets were sintered in oxygen at 200 °C for 12 hours. Glass was used as substrates for growing these Mg<sub>x</sub>Zn<sub>1-x</sub>O thin films. The substrates have the thickness of 1 mm . Before loaded into the vacuum chamber, substrates were cleaned with standard chemical method, by which the substrate was first cleaned in acetone and then cleaned in methanol for 10 min in ultrasonic bath. Thin films were grown in oxygen environment with O<sub>2</sub> partial pressure of (10<sup>-1</sup> mbar) at substrate temperature of 250 °C. Laser energy density focused on the target was about (0.5-1) J/cm<sup>2</sup>. The deposition time was typically 10 min. After the deposition, thin films were cooled down to room temperature.

The absorption and transmission spectra of Mg<sub>x</sub>Zn<sub>1-x</sub>O thin films were studied by UV-visible spectroscopy at room temperature in the range (200-900) nm. The topography of the Mg<sub>x</sub>Zn<sub>1-x</sub>O surface was inspected with optical transmission-microscope (OTM) .

The data from transmission spectrum could used in the calculation of the absorption coefficient (α) by using the following equation[14]:

$$\alpha = \frac{1}{d} \ln \frac{1}{T} \quad \dots\dots(1)$$

Where d: is the thickness of thin film, and T is the transmission.

The absorption coefficient (α) and optical energy gap (Eg) are related by [15]:

$$\alpha h\nu = A(h\nu - E_g)^{1/2} \quad \dots\dots(2)$$

Where A: is constant depending on transmission probability, h: is Plank's constant , ν: is the frequency of the incident photon, Eg: is the energy gap of the material.

Both transmittance (T) and absorbance (A) were converted to reflectance values (R), in terms of (R+A+T=1).

The reflectance can be expressed in terms of optical constants, (n) and (K) as [16]:

$$R = \frac{(n-1)^2 + k^2}{(n+1)^2 + k^2} \quad \dots\dots(3)$$

Where n is the refractive index and (K) is the extinction coefficient.

The complex dielectric constant is given by the following equation [17] :

$$\epsilon = \epsilon_r + i\epsilon_i = (n + iK)^2 \quad \dots\dots(4)$$

Where ε<sub>r</sub> , and ε<sub>i</sub> are the real and imaginary parts of ε and (n+iK)<sup>2</sup> is the complex refractive index. From equation (3) we obtain:

$$\epsilon_r = n^2 + K^2, \text{ and } \epsilon_i = 2nK \quad \dots\dots(5)$$

The crystalline structure of the films was characterized by X-ray diffraction measurement using

Philips PW 1050,  $\lambda=1.54 \text{ \AA}$  from Cu - K $\alpha$  radiation.

### 3.Results and discussion

Figure (1) shows transmittance spectra for Mg<sub>x</sub>Zn<sub>1-x</sub>O films grown at various Mg concentration in the targets (x). The transmission spectra of the films indicate: (1) optical transparency over 85% including the film grown at x=0.15, (2) oscillations in their transmittance, (3) shift of the absorption edge to lower wavelength with increase in Mg concentration (x), and (4) a sharp absorption edge for all as-grown MgZnO alloys films.

The data from transmission spectrum are used to calculate absorption coefficient by using equation (1). Figure (2) shows the variation in optical absorption spectra for the Mg<sub>x</sub>Zn<sub>1-x</sub>O films for different Mg concentration. It is clear that the films have high absorption coefficient at short wavelength range ( $\alpha=1.3 \times 10^5 \text{ cm}^{-1}$  for  $\lambda < 350 \text{ nm}$ ), then decrease at different rates dependence on the film structure to reach constant values at long wavelengths ( $\alpha=2 \times 10^4 \text{ cm}^{-1}$  for  $\lambda > 355 \text{ nm}$ ), where the films become transparence at this wavelengths.

The energy gap values depends in general on the film crystal structure, the arrangement and distribution of atoms in the crystal lattice, also it is affected by crystal regularity. The energy gap (E<sub>g</sub>) value is calculated by extrapolation of the straight line of the plot of  $(\alpha h\nu)^2$  versus photon energy for different Mg concentration in the target (x) as shown in Figure (3). The linear dependence of  $(\alpha h\nu)^2$  with  $(h\nu)$  indicates direct band gap. The band gap increases with the increase in Mg concentration (x) in the target as

shown in Figure (4). The surface morphology from optical microscope studies shown in Figure (5), which show more homogeneous in surface as the Mg concentration increase.

Figure (6) shows the X-ray diffraction (XRD) pattern of the films deposited at substrate temperature 250°C for Mg<sub>x</sub>Zn<sub>1-x</sub>O (at x=0.3) and pure ZnO (x=0) thin films. We see that the Full Width at Half Maximum (FWHM) for X-ray curve of Mg<sub>0.3</sub>Zn<sub>0.7</sub>O peak was greater than that of ZnO peak and there was a slightly shift to higher diffraction angle (2 $\theta$ ) with increasing (x) which have hexagonal structure corresponds to (002) orientation [18]. The parameters of the XRD growth process are listed in table 1.

The refractive indices of Mg<sub>x</sub>Zn<sub>1-x</sub>O films for x=0.15, 0.2 and 0.3 as functions of wavelength are plotted in figure (7). This figure reveals that the expo behavior the films were deposited at different Mg content. It can be seen that as Mg concentration (x) increases, the values of (n) decreases. One is the optical loss caused by absorption and scattering, which decreases the amplitudes of the transmission intensity oscillations at shorter wavelengths, in this work it can be neglected because for the highly transparent Mg<sub>x</sub>Zn<sub>1-x</sub>O films. In the determination of refractive indices for the Mg<sub>x</sub>Zn<sub>1-x</sub>O films, the main loss arises from the transmission measurement procedures, such as small difference of light spot sizes and apertures.

Figure(8) shows the extinction coefficient for Mg<sub>x</sub>Zn<sub>1-x</sub>O films grown at various Mg concentration (x=0.15, 0.2 and 0.3) as a function of photon energy. The extinction coefficient represents the amount of

attenuation of an electromagnetic wave that is traveling in material, where its value depends on the density of free electrons in the material and also on the structure nature. The values of extinction coefficient are directly related to the absorption of light. It can be noticed that there is a slight increase of extinction coefficient values at higher energies. After that, there is an increase with increasing photon energy and this is a general behavior. Figures (9) and (10) show the variation of real part and imaginary part of dielectric constant respectively as a function of photon energy. Where real part ( $\epsilon_r$ ) is the normal dielectric constant which represents the amount of actual saving of electrical energy and the imaginary part ( $\epsilon_i$ ) represents the absorption loss associated with free carriers. Two parts of complex dielectric constant were calculated using the relations (5). The curves for both parts are found to be oscillatory in nature depending upon the crystal structure and the thickness of the film. Where the values of real part undergoes rising and falling.

#### 4. Conclusions

The bandgap was increased with increase of Mg concentration from 3.3eV to 4.2eV as well as with the change of thickness. The absorption edge was found to shift toward lower wavelength with increase in Mg (x) value. X-ray diffraction studies show that the Mg<sub>x</sub>Zn<sub>1-x</sub>O film has singlecrystalline structure (hexagonal) correspond to (002) orientation, and there is a slightly shifted to larger 2 $\theta$  angle with increasing x from (x=0 to x=0.3). The refractive index decreases with increasing Mg concentration x.

#### References

- [1] S. Cho, J. Ma, Y. Kim, Y. Sun, G.K.L. Wong and J.B. Ketterson, Appl. Phys. Lett., **75**, 2761 (1999).
- [2] G. H. Lee, T. Kawazoe and M. Ohtsu, Appl. Surf. Sc., **239**, 394 (2005).
- [3] Z. K. Tang, G. K. L. Wang, P. Yu, M. Kawasaki, A. Ohtomo, H. Koinuma and Y. Segawa, Appl. Phys. Lett., **72**, 3270 (1998).
- [4] A. Ohtomo, K. Tamura, M. Kawasaki, T. Makino, Y. Segawa, Z.K. Tang, G.K.L. Wong, Y. Matsumoto and H. Koinuma, Appl. Phys. Lett., **77**, 2204 (2000).
- [5] T. Makino, Y. Segawa, M. Kawasaki, A. Ohtomo, R. Shiroki, K. Tamura, T. Yasuda and H. Koinuma, Appl. Phys. Lett., **78**, 1237 (2001).
- [6] T. Gruber, C. Kirchner, R. Kling, F. Reuss, and A. Waag, Appl. Phys. Lett. **84**, 5359 (2004).
- [7] T. Makino, C. H. Chia, N. T. Tuan, Y. Segawa, M. Kawasaki, A. Ohtomo, K. Tamura, and H. Koinuma, Appl. Phys. Lett. **77**, 1632 (2000).
- [8] T. Gruber *et al.*, Appl. Phys. Lett. **83**, 3290 (2003).
- [9] R. Schmidt-Grund *et al.*, Thin Solid Films **455–456**, 500 (2004).
- [10] M. Lorenz *et al.*, Appl. Phys. Lett. **86**, 143113 (2005).
- [11] S. Choopun, R. D. Vispute, W. Yang, R. P. Sharma, T. Venkatesan, and H. Shen, Appl. Phys. Lett. **80**, 1529 (2002).
- [12] B. Amrani, Rashid Ahmed, F. El Haj Hassan, Computational Materials Science **40**, 66-72 (2007).
- [13] Wei Wei, Chunming Jin, Anand Doraiswamy, Roger J Narayan, and Jagdish Narayan, Mater. Res. Soc. Symp. Proc. Vol. 957 (2007).
- [14] S.M. Sze, "Physics of Semiconductor Devices", Second

edition, Jon Wiley and Sons, New York, (1981).

[15] S. Dimitrijevic, "Understanding Semiconductor Devices", Copyright by Oxford University Press, (2000).

[16] F.I.Ezema, Ph.D. The pacific J. of Science and Technology, 6(1), (2005), 6-14.

[17] D.D.O.Eya, A.J.Ekponobi, and C.E.Okeke, The pacific J. of Science and Technology, 6(2), (2005), 98-104.

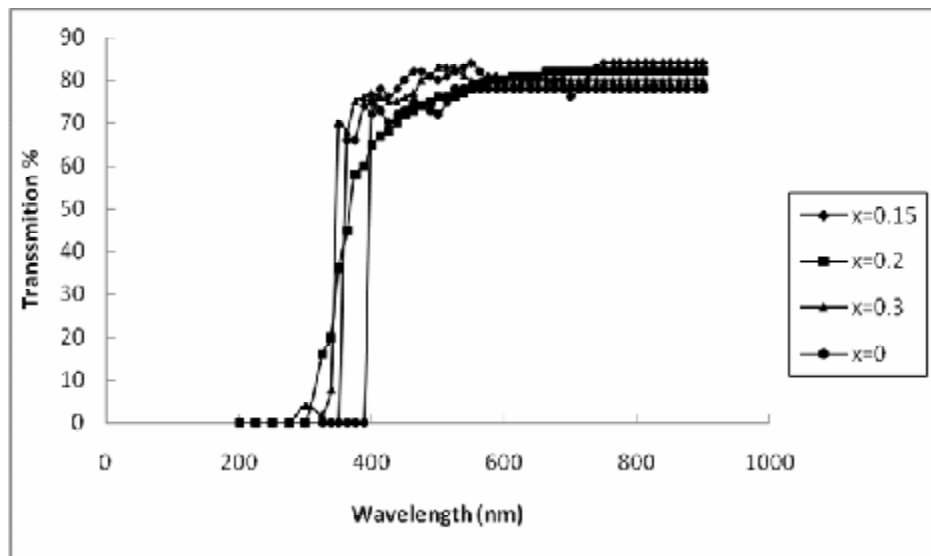
[18] W.I.Park, Gyu-Chul Yi, and H.M.Jang, Appl. Phys. Lett., **79**, 13, 2022 (2001).

[19] P. Bhattacharya, Rasmi R. Das, Ram S. Katiyar, Thin Solid Films **447-448**, 564-567 (2004).

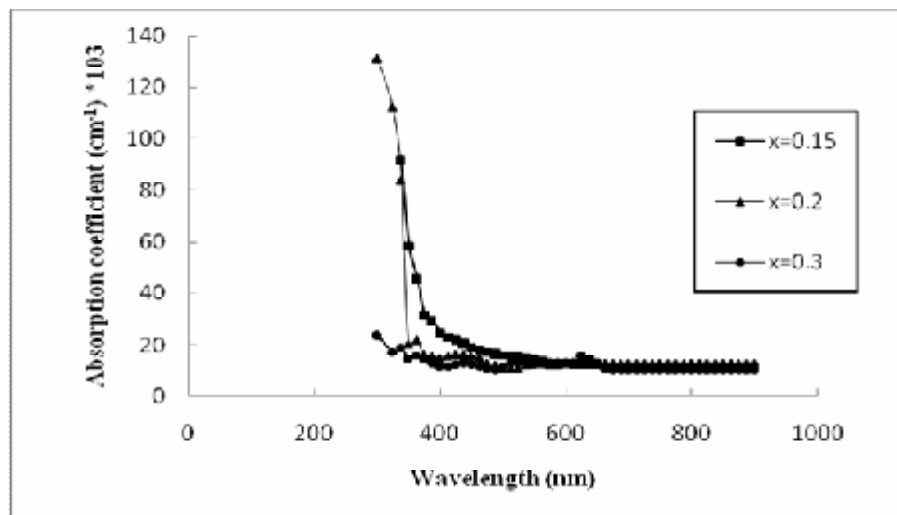
[20] Yinzhu Zhang, Junhui He, Zhizhen Ye, Lu Zou, Jingyun Huang, Liping Zhu, Binghui Zhao, Thin Solid Films **458**, 161-164 (2004)

Table (1) XRD growth parameters

Samples	orientation	Diffraction angle ( $2\theta$ )
ZnO	002	34
$Mg_{0.3}Zn_{0.7}O$	002	34.8
MgO	111	36.6

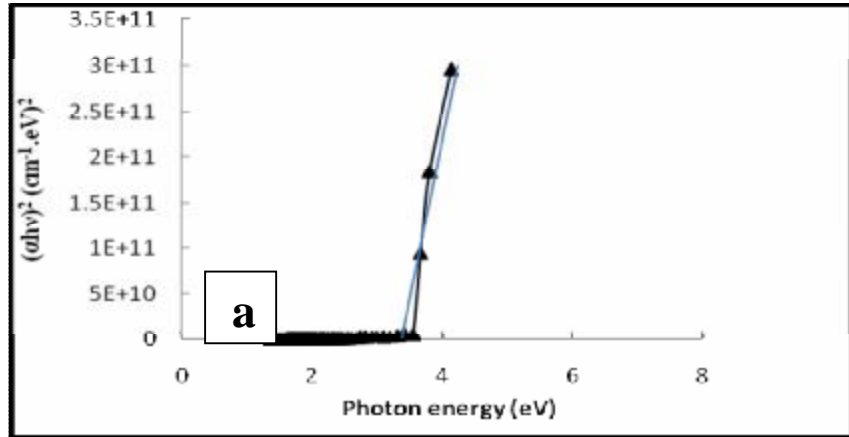


Figure(1) Optical transmission of  $Mg_xZn_{1-x}O$  films grown at 250 °C with different x

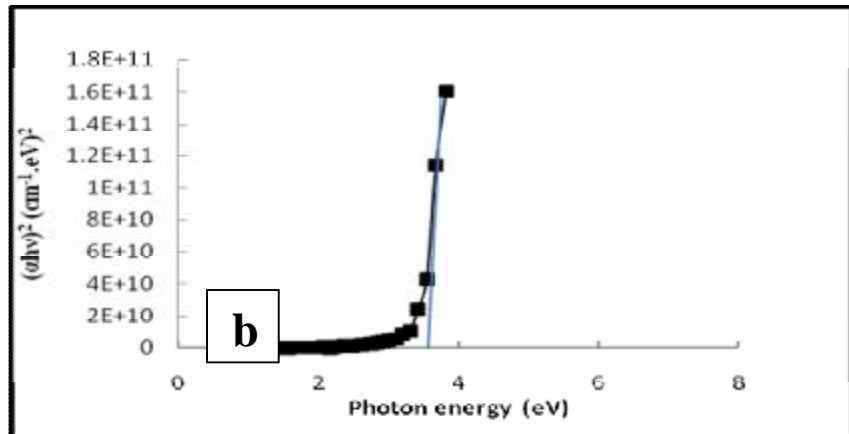


Figure(2) The optical absorption coefficient spectra for the  $Mg_xZn_{1-x}O$  films for different Mg concentration (x).

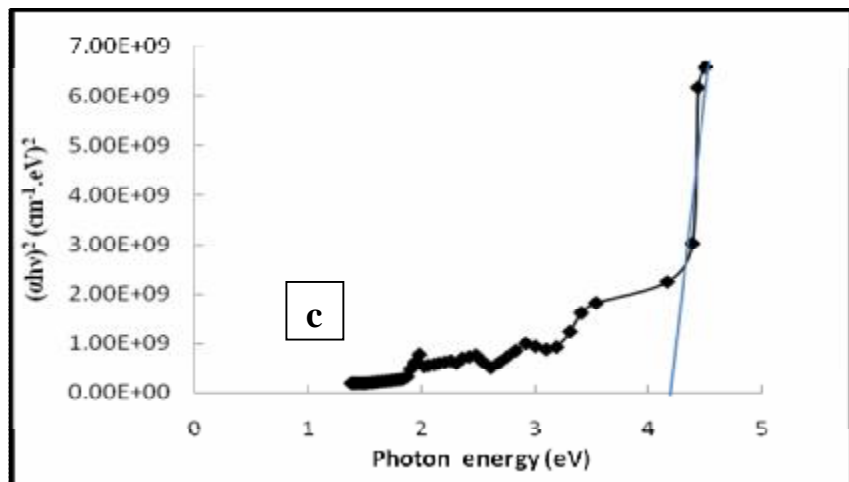
(a)  $x=0.15$



b)  $x=0$ .

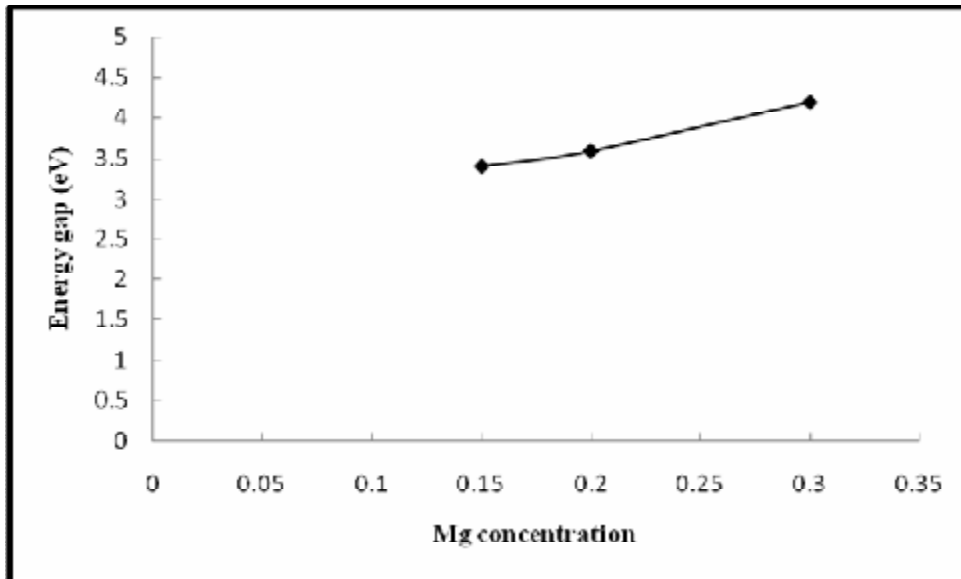


(c)  $x=0.3$

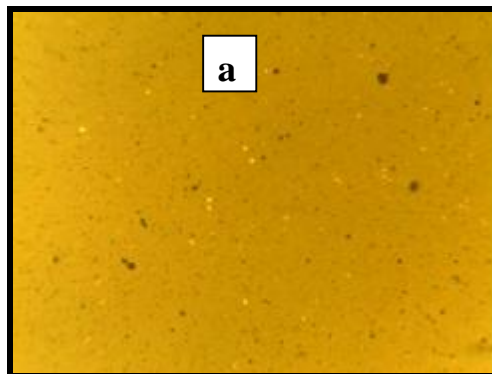


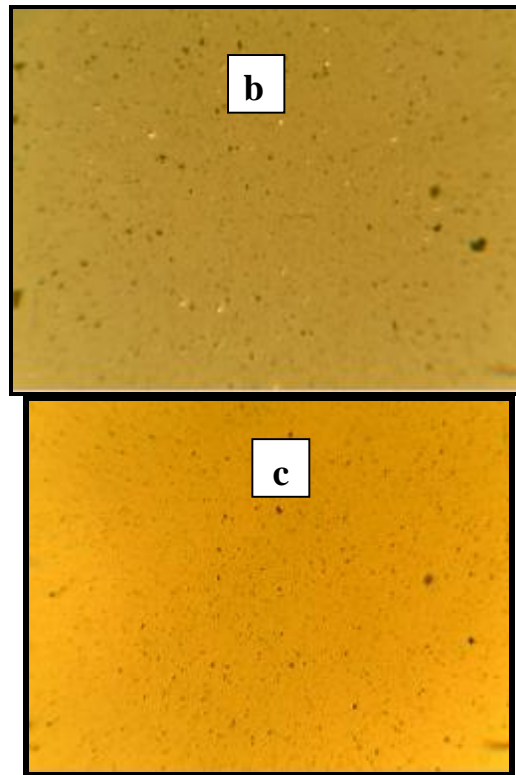
Figure(3) A plots of  $(\alpha h\nu)^2$  verses photon energy ( $h\nu$ ) of  $Mg_xZn_{1-x}O$  thin films for different ( $x$ ) .



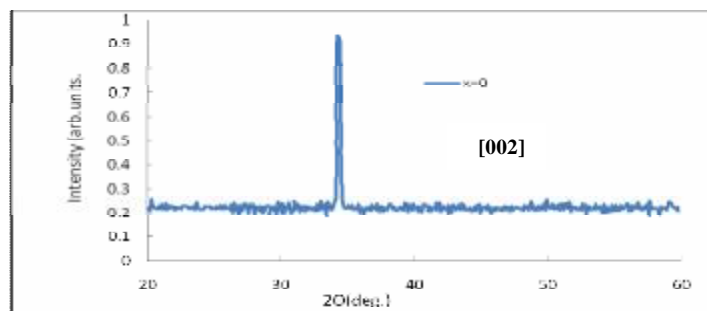


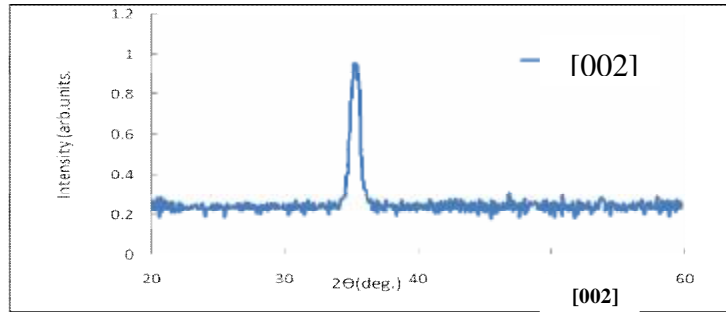
Figure(4) Band gap energy as a function of Mg concentration in the target



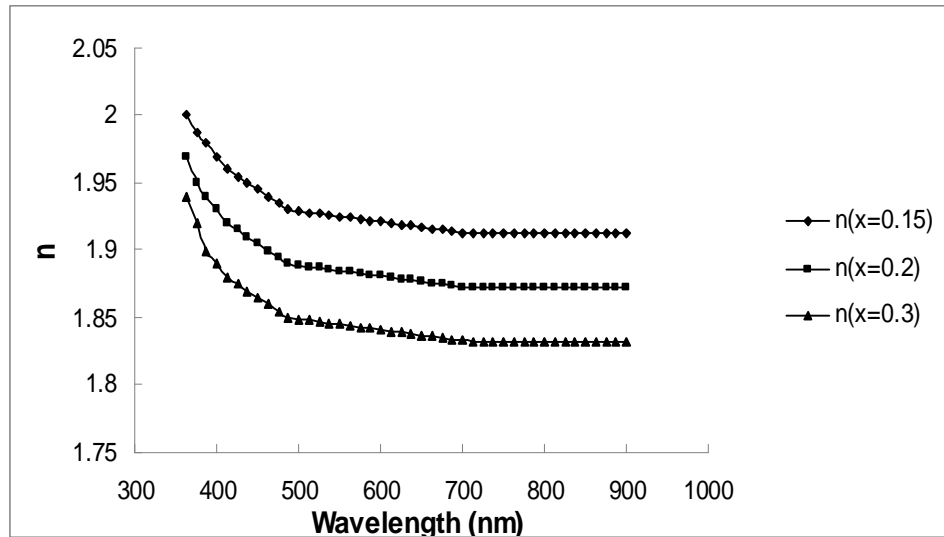


Figure(5) The surface morphology of  $Mg_xZn_{1-x}O$  thin film with different Mg concentration (x):  
(a)  $x=0.15$  (b)  $x=0.2$  (c)  $x=0.3$

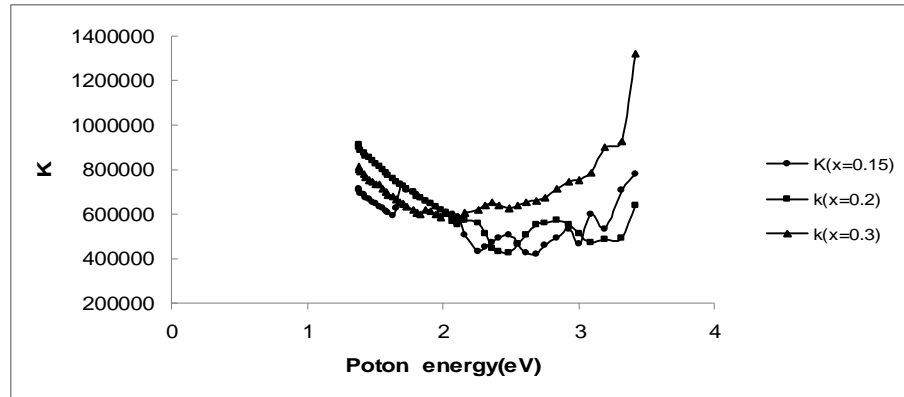




Figure(6) XRD pattern of  $Mg_xZn_{1-x}O$  thin films for ( $x=0$  and  $x=0.3$ )



Figure(7) The refractive indices of  $Mg_xZn_{1-x}O$  films ( $x=0.15, 0.2,$  and  $0.3$ )



Figure(8) The extinction coefficient (K) for  $Mg_xZn_{1-x}O$  films as a function of photon energy.

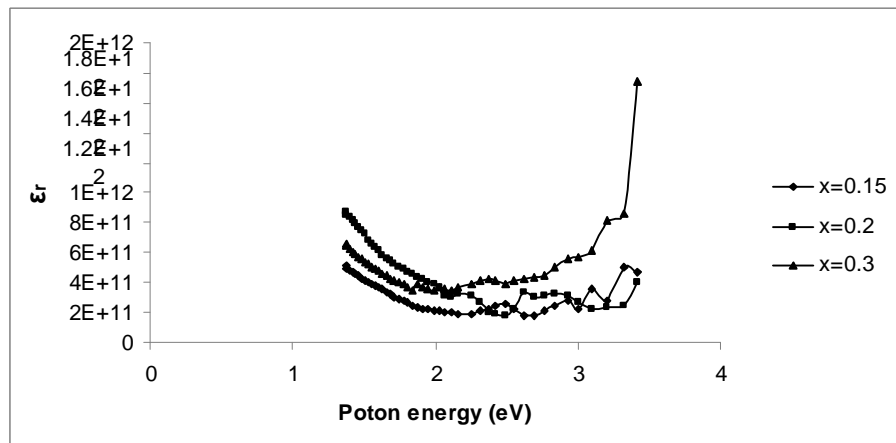
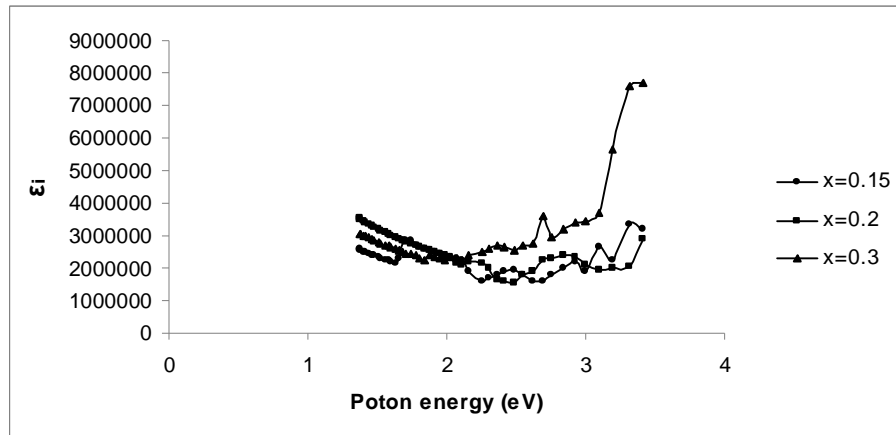


Figure (9) Real part of dielectric constant for  $Mg_xZn_{1-x}O$  films as a function of photon energy.



Figure(10) imaginary part of dielectric constant for  $Mg_xZn_{1-x}O$  films as a function of photon energy.